Vesicular Zinc Promotes Presynaptic and Inhibits Postsynaptic Long-Term Potentiation of Mossy Fiber-CA3 Synapse

Citation: Pan, Enhui, Xiao-an Zhang, Zhen Huang, Artur Krezel, Min Zhao, Christine E. Tinberg, Stephen J. Lippard, and James O. McNamara. "Vesicular Zinc Promotes Presynaptic and Inhibits Postsynaptic Long-Term Potentiation of Mossy Fiber-CA3 Synapse." Neuron 71, no. 6 (September 2011): 1116–1126. © 2011 Elsevier Inc.

As Published: http://dx.doi.org/10.1016/j.neuron.2011.07.019

Publisher: Elsevier

Persistent URL: http://hdl.handle.net/1721.1/95813

Version: Final published version: final published article, as it appeared in a journal, conference proceedings, or other formally published context

Neuron
Article

Vesicular Zinc Promotes Presynaptic and Inhibits Postsynaptic Long-Term Potentiation of Mossy Fiber-CA3 Synapse

Enhui Pan,[1,6] Xiao-an Zhang,[4,6] Zhen Huang,[4] Artur Krezel,[5] Min Zhao,[4] Christine E. Tinberg,[4] Stephen J. Lippard,[4,7,*] and James O. McNamara[1,2,3,8,*]
[1]Department of Medicine (Neurology)
[2]Department of Neurobiology
[3]Department of Pharmacology and Molecular Cancer Biology
Duke University Medical Center, Durham, NC 27710, USA
[4]Department of Chemistry, Massachusetts Institute of Technology, Cambridge, MA 02139, USA
[5]Laboratory of Protein Engineering, University of Wroclaw, 50-137 Wroclaw, Poland
[6]These authors contributed equally to this work
[7]Present address: Department of Chemistry, 18-498, Massachusetts Institute of Technology, Cambridge, MA 02139, USA
[8]Present address: Department of Neurobiology, Campus Box 3676, Duke University Medical Center, Durham, NC 27710, USA
*Correspondence: lippard@mit.edu (S.J.L.), jmc@neuro.duke.edu (J.O.M.)
DOI 10.1016/j.neuron.2011.07.019

SUMMARY

The presence of zinc in glutamatergic synaptic vesicles of excitatory neurons of mammalian cerebral cortex suggests that zinc might regulate plasticity of synapses formed by these neurons. Long-term potentiation (LTP) is a form of synaptic plasticity that may underlie learning and memory. We tested the hypothesis that zinc within vesicles of mossy fibers (mf) contributes to mf-LTP, a classical form of presynaptic LTP. We synthesized an extracellular zinc chelator with selectivity and kinetic properties suitable for study of the large transient of zinc in the synaptic cleft induced by mf stimulation. We found that vesicular zinc is required for presynaptic mf-LTP. Unexpectedly, vesicular zinc also inhibits a form of postsynaptic mf-LTP. Because the mf-CA3 synapse provides a major source of excitatory input to the hippocampus, regulating its efficacy by these dual actions, vesicular zinc is critical to proper function of hippocampal circuitry in health and disease.

INTRODUCTION

The discovery of high levels of zinc in synaptic vesicles of neurons within the mammalian cerebral cortex (Maske, 1955) has intrigued and puzzled both neuroscientists and zinc biologists for over half a century (note: the term "zinc" will be used to refer to free or loosely bound zinc). Its localization to synaptic vesicles provided strong circumstantial evidence for its release, yet the functional consequences of zinc release remain incompletely understood. The curious localization of zinc to axons of cortical glutamatergic neurons, in particular to neurons that form connections within the same cerebral hemisphere, suggested that vesicular zinc regulates plasticity of synapses formed by these excitatory neurons.

Long-term potentiation (LTP) is a form of synaptic plasticity that provides a plausible cellular mechanism underlying learning and memory (Bliss and Collingridge, 1993; Malinow and Malenka, 2002). Two major forms have been distinguished: (1) an NMDA receptor-dependent form in which key events underlying both expression and induction reside postsynaptically and (2) an NMDA receptor-independent form, also known as mossy fiber LTP (mf-LTP), in which mechanisms underlying expression are located presynaptically, but for which the site of induction is controversial (Henze et al., 2000; Nicoll and Schmitz, 2005). Studies of the contribution of vesicular zinc to LTP have centered on mf-LTP because of the high concentrations of zinc in mf axons, where it is both colocalized and coreleased with glutamate (Haug, 1967; Frederickson et al., 2005; Qian and Noebels, 2005).

Despite extensive study, whether or not zinc contributes to mf-LTP remains controversial. Application of different membrane-permeable zinc chelators (see Figure S1 available online) led to contradictory observations (Budde et al., 1997; Quinta-Ferreira and Matias, 2004). Thus far, CaEDTA has been the main cell-impermeable metal chelator employed to study zinc and mf-LTP. Acute application of 2.5 mM CaEDTA promoted mf-evoked NMDA receptor-mediated EPSCs yet failed to attenuate mf-LTP (Vogt et al., 2000); however, higher concentrations of CaEDTA inhibited mf-LTP (Li et al., 2001; Huang et al., 2008). Importantly, studies of a mutant mouse, *mocha*, which exhibits reduced amounts of vesicular zinc in mf axons, revealed persistence of mf-LTP, arguing against a role for zinc in mf-LTP (Vogt et al., 2000).

We reasoned that these contradictory results might be due in part to shortcomings of existing zinc chelators. To block the effects of synaptically released zinc efficiently, while minimizing disruption of its pleiotropic intra- and extracellular functions, an ideal zinc chelator should be water soluble and cell membrane impermeable. Such a chelator should bind zinc selectively with respect to other abundant metal ions, a property lacking in CaEDTA, which has appreciable affinity for calcium and

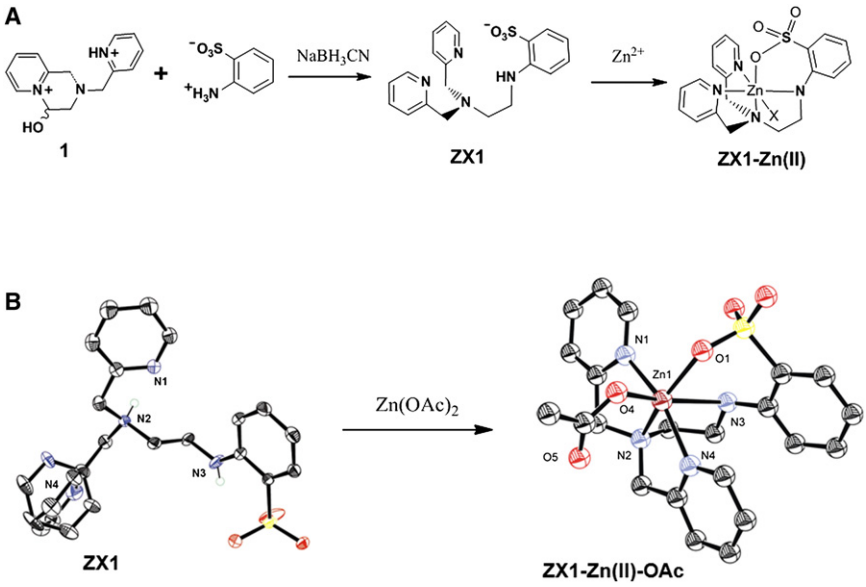

Figure 1. Synthesis and X-ray Structures of ZX1 and Its Zinc Complex

(A) Using the intramolecular pyridinium salt 1 as a synthetic precursor for installing the DPA unit, ZX1 was prepared by reductive amination with 2-sulfonated aniline.

(B) X-ray structure of ZX1 (left), displaying the two orientations of the disordered pyridine ring refined at 50:50 occupancy. Hydrogen atoms, except those on N2 and N3, are omitted for clarity; X-ray structure of ZX1-Zn(II)(OAc) (right). Hydrogen atoms are omitted for clarity.

See also Figure S2.

magnesium as well as zinc. Finally, given the short lifetime of high concentrations of zinc within the synaptic cleft following its release, the chelator must bind zinc rapidly. To address these requirements, we designed the zinc chelator, ZX1 (Figure 1A). Here, we report its preparation and characterization and describe its use in studying mf-LTP. The results reveal that vesicular zinc is required for induction of presynaptic mf-LTP and, unexpectedly, also masks induction of a novel form of postsynaptic mf-LTP.

RESULTS

Design and Synthesis of ZX1

In pursuit of an extracellular chelator that would provide the desired properties described above, we designed ZX1 (Figure 1). The zinc binding subunit, a dipicolylamine (DPA), reprises the high selectivity for zinc over calcium and magnesium previously developed (Burdette et al., 2001; Chang and Lippard, 2006; Zhang et al., 2007). We introduced the negatively charged sulfonate group to render the compound membrane impermeable and to facilitate rapid zinc binding by improving the electrostatic interaction compared to DPA itself. The electron deficient aniline moiety lowers the pK_a of the adjacent nitrogen atom, which also favors rapid zinc binding. A protonated nitrogen atom would have to lose H^+ prior to coordination, a process that slows down metal chelate formation. Thus, ideally, the chelator would not be protonated at physiological pH, a condition favored by a pK_a value below ~7. The aniline nitrogen atom and the ortho sulphonate group are both expected to participate in zinc binding, but not to significantly affect zinc affinity, because both are weak ligands.

Zinc Binding and Selectivity Studies

ZX1 readily forms a 1:1 zinc complex in the solid state and in solution upon addition of one equivalent of $Zn(OAc)_2$, as revealed by X-ray crystallography (Figure 1) and ^{1}H-NMR spectroscopy, details of which may be found in Supplemental Information and Figure S2, available online. Because the protonation states of a metal-binding chelator can affect the rate of metal chelate formation, we determined these properties (Figure S3A). The electron-withdrawing effect of the sulfonated aniline motif facilitates rapid binding of zinc to ZX1 by lowering the pK_a of the most basic tertiary nitrogen (Figure 1). The pH titration curve shifted significantly upon addition of one equivalent of $ZnCl_2$ to a solution of ZX1 (Figure 2A). For comparison, little change occurred with a large excess (100 equiv.) of Ca(II) or Mg(II), reflecting the high selectivity of ZX1 for Zn(II) over these biologically relevant metal ions (Figure S3B). This result is in agreement with the high Zn(II)-selectivity of DPA as observed in Zinpyr zinc sensors. From the two titration curves we derived a dissociation constant (K_d) of 1.0 nM (Table S2).

Having demonstrated the high affinity and selectivity of ZX1 for zinc, we next investigated the metal binding kinetics of the chelator. In these experiments, we took advantage of the fluorescent zinc sensor, ZP3 (Chang et al., 2004), which responds rapidly to changes of zinc concentration in solution with well-established kinetic parameters (Nolan et al., 2005). ZP3 alone is weakly fluorescent, and its fluorescence increases upon formation of a 1:1 complex with zinc (Chang et al., 2004). When added to a preformed ZP3-Zn(II) (1:1) solution, the zinc chelators induced an instantaneous reduction of fluorescence intensity due to the loss of the zinc via competitive binding. The rate of the fluorescence decrease reflects the rate of the zinc binding by chelators. The slope of the fluorescence decrease (Figure 2B) reveals that ZX1 binds zinc much more rapidly than CaEDTA; ZX1 binds zinc even more rapidly than TPEN (see Figure S4B), the most widely used intracellular zinc chelator.

These results led us to compare the effects of ZX1 and CaEDTA on the high yet fleeting concentration of zinc in the synaptic cleft induced by activation of the mf. Zinc is known to inhibit the NMDA subtype of glutamate receptor by both a low- and high-affinity mechanism (Paoletti et al., 1997; Traynelis et al.,1998; Choi and Lipton, 1999). Because mf activation evokes simultaneous release of both glutamate and zinc, chelation of synaptically released zinc would be expected to increase the amplitude of NMDA EPSC (I_{NMDA}). CaEDTA (2.5 mM) was previously found to disinhibit the synaptically evoked low-affinity

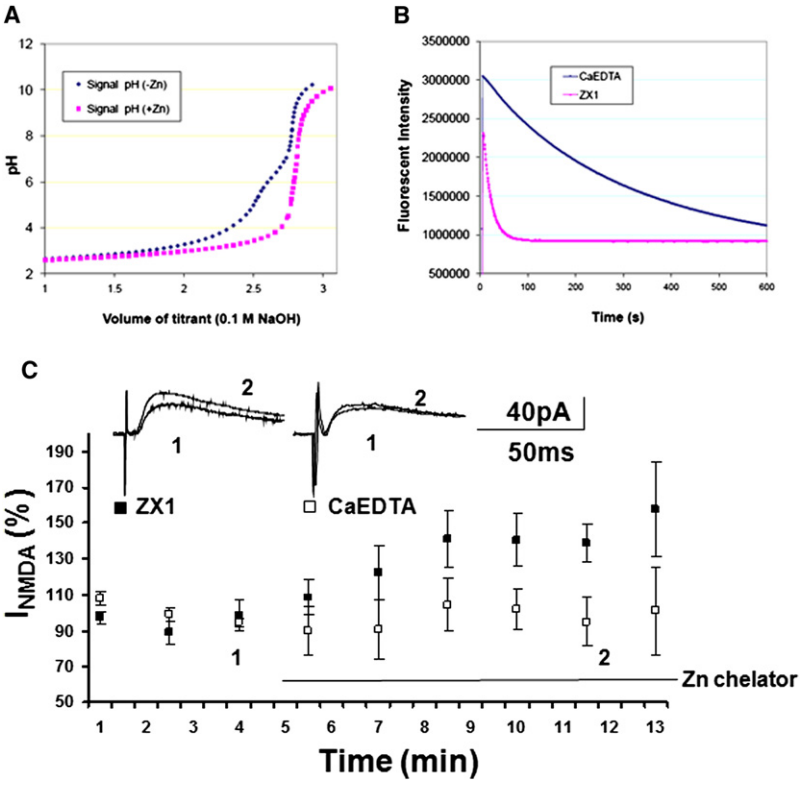

Figure 2. Zinc-Binding and Fluorescence Quenching Properties of ZX1

(A) The experimental potentiometric equilibrium curves for free ZX1 (blue) and ZX1/Zn(II) (1:1) complex (magenta) as a function of added titrant (0.1 M NaOH). See also Figure S3.

(B) Fluorescence quenching of a 1.67 μM solution of ZP3-Zn(II) (1:1) by zinc chelators in pH 7.0 buffer (50 mM PIPES, 100 mM KCl). ZX1 (magenta) binds zinc more rapid than CaEDTA (blue). See also Figure S4.

(C) ZX1 (100 μM), but not CaEDTA (7.5 mM), inhibits the NMDA receptor mediated EPSC (I_{NMDA}) evoked in CA3 pyramids by mf stimulation (0.033 Hz). Pharmacologically isolated synaptic I_{NMDA} were recorded in CA3 pyramids at a holding potential of +30 mv. Representative traces from ZX1 (left) and CaEDTA (right) reflect averages of responses to stimulations at 30 second intervals during 5 min epochs immediately before (1) and between 3 and 8 min after (2) application of each chelator to the bath (denoted by horizontal line). ZX1 produced a 40% ± 13% increase of I_{NMDA} (n = 6 cells, p = 0.02, paired t test) whereas CaEDTA produced no significant increase (3% ± 17%, n = 5 cells, p > 0.05).

but not the high-affinity I_{NMDA}; the inability of CaEDTA to disinhibit the high affinity synaptic I_{NMDA} was attributed to its slow rate of chelating zinc (Vogt et al., 2000). We assessed pharmacologically isolated I_{NMDA} responses of CA3 pyramidal cells to mf stimulation in whole-cell recordings at a positive holding potential (+30 mV) (Figure 2C). Inclusion of CaEDTA (7.5 mM) produced no significant change in the synaptically evoked I_{NMDA} (Figure 2C), confirming and extending previous observations (Vogt et al., 2000). By contrast, inclusion of ZX1 (100 μM) enhanced the synaptically evoked I_{NMDA} by approximately 40% (Figure 2C), supporting the conclusion that ZX1 rapidly chelates the high yet fleeting concentration of zinc within the synaptic cleft induced by a single action potential invading the mf. Together with its selectivity and membrane impermeability (Figure S4C), the rapidity with which ZX1 chelates zinc renders it a valuable tool with which to examine the functional consequences of zinc released by HFS of the mf.

Effects of ZX1 on Plasticity of the Mossy Fiber-CA3 Pyramid Synapse

LTP was induced by HFS of the mf in acutely isolated mouse hippocampal slices (Figure 3, top panels). The amplitude of the mf-evoked field excitatory postsynaptic potential (fEPSP) was recorded from the CA3 pyramidal cell population in the presence of vehicle or bath-applied ZX1. With vehicle, HFS of the mf induced LTP, as revealed by an increase of fEPSP magnitude of 149% ± 9% when measured 50–60 min after compared to the 10 min immediately preceding HFS (Figure 3, top left). The effects of ZX1 were concentration dependent, with some inhibition detectable at 50 μM; similar effects were obtained with 100 and 200 μM levels of ZX1, the inhibition approximating 60% of maximum (Figure 3, top right). Notably, ZX1 did not affect baseline transmission of the mf-CA3 pyramid synapse (Figure S6).

A hallmark of mf-LTP is that increased P_r of glutamate from mf terminals underlies its expression (Zalutsky and Nicoll, 1990; Weisskopf and Nicoll, 1995; Tong et al.,, 1996; Reid et al., 2004). To examine the role of zinc in the induction of mf-LTP, additional experiments were performed using whole-cell recordings of CA3 pyramids to analyze the effects of ZX1 while simultaneously assessing paired pulse facilitation (PPF). PPF is a form of presynaptic plasticity consisting of the enhancement of transmitter release in response to the second of two stimuli delivered at a short interval (e.g., 20–100 ms; Regehr and Stevens, 2001). PPF is normally inversely correlated with P_r, such that synapses with low P_r show larger PPF than synapses with higher P_r. PPF was measured by applying a pair of pulses of stimulus intensity 30% that of maximum EPSC with a 60 ms interstimulus interval, and was defined as the amplitude of the EPSC evoked by pulse #2 divided by the amplitude of the EPSC evoked by pulse #1 (Figure 3B, bottom left). HFS of the mossy fibers in the presence of vehicle induced an increase of the EPSC amplitude of 188% ± 16% (n = 8) (Figure 3, middle left). A significant reduction of PPF was evident 10–20 min following HFS (1.3 ± 0.1) compared to baseline levels prior to HFS (2.8 ± 0.5, p = 0.001, paired t test), confirming previous findings (reviewed in Nicoll and Schmitz, 2005; Figure 3, bottom left). Inclusion of 100 μM ZX1 in the bath reduced the HFS-induced increase of the EPSC (131% ± 21%, n = 9, p = 0.04 versus vehicle; Figure 3, middle right). ZX1 also prevented the HFS-induced reduction of PPF (before HFS 3.1 ± 0.5; after HFS 2.7 ± 0.7, t test p = 0.8; Figure 3, bottom right). Because PPF is a surrogate measure of P_r, this result implies that zinc is

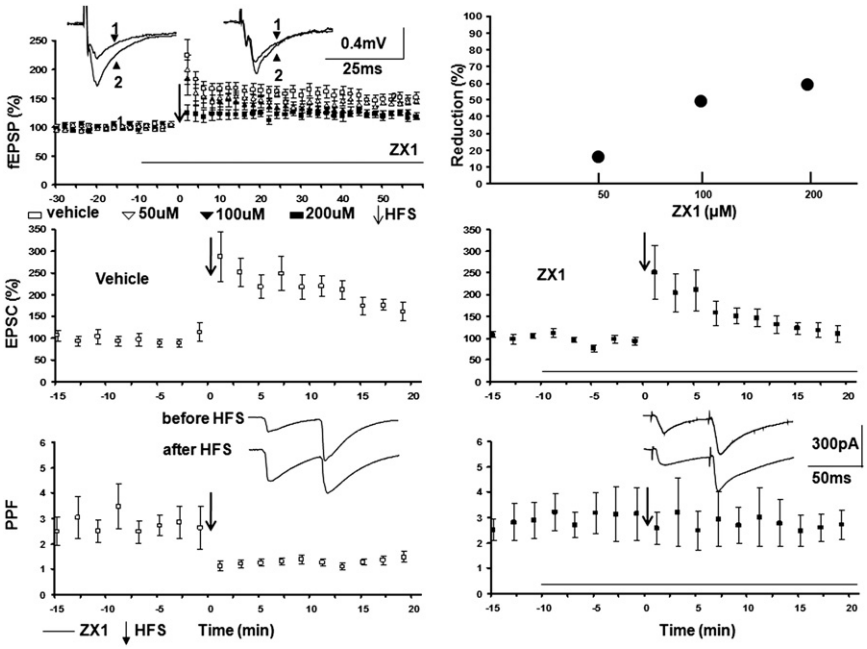

Figure 3. ZX1 Inhibits Induction of LTP at the MF-CA3 Synapse

Top left: Field EPSPs (fEPSPs) were recorded from hippocampal slices acutely isolated from WT mice (P28–P42) and the effects of ZX1 were examined on LTP of mf-CA3 synapse. Representative traces from vehicle (left) and 100 μM ZX1 (right) are averages of responses collected during 10 min prior to HFS (1) and between 50 and 60 minutes following HFS (2). Arrow denotes the timing of application of HFS and arrowheads denote the baseline fEPSP (1) and fEPSP after HFS (2). Horizontal line denotes timing of application of ZX1 to bath. Top right: Reduction of LTP induced by HFS is plotted as function of increasing concentrations of ZX1. Plot is based upon the following results: compared to baseline, vehicle 149 ± 9 (n = slices from 10 mice); ZX1 50 μM 142% ± 3% (n = 4); ZX1 100 μM 124% ± 3% (n = 7); ZX1 200 μM 120% ± 5% (n = 8). Middle and bottom panels: whole-cell recordings of CA3 pyramids were performed in hippocampal slices acutely isolated from WT mice (P21–P29) and the effects of ZX1 (100 μM) were examined on LTP and PPF of mf-CA3 synapse following HFS of the mossy fibers. Percent potentiation induced by HFS (middle left and right): vehicle 188 ± 16 (n = 8); ZX1 100 μM 131% ± 21% (n = 9). PPF before and after HFS (bottom left and right): vehicle 2.8 ± 0.5 and 1.3 ± 0.1 respectively, (paired t test, p = 0.04); ZX1 3.1 ± 0.8 and 2.7 ± 0.7, respectively, (paired t test, p = 0.2). Representative traces from Vehicle (left) and ZX1 (right) before and after HFS. Arrows denote administration of HFS. Horizontal lines in right middle and bottom panels denote timing of application of ZX1 to bath. The representative traces are averages of responses collected at intervals of 30 seconds for the 10 minutes preceding HFS (before) and the last 10 minutes of the recording following HFS (after); the interval between the pair of stimulations was 60 msec. Values represent mean ± standard error of the mean. See also Figure S5.

required for induction of this plasticity of the presynaptic terminal. The ZX1-mediated inhibition of mf-LTP and the decrease of PPF following HFS were confirmed in additional experiments performed with field potential recordings (Figure S5B).

Although ZX1 inhibits mf-LTP, the foregoing experiments do not address whether ZX1 inhibits the induction and/or expression of LTP. Because ZX1 was added to the bath 10 min prior to HFS and remained for the duration of the experiment, inhibition of LTP by ZX1 could be mediated either by preventing induction of LTP or simply by masking expression of LTP following its induction. To distinguish between these possibilities, ZX1 (100 μM) was added to the bath 30 min following HFS and allowed to remain there for an additional 30 min (Figure S5C). The magnitudes of the fEPSP and PPF were determined for a 10 min epoch immediately prior to addition of ZX1, and these values were compared to fEPSP and PPF magnitudes during the 10 min epoch between 20 and 30 min following ZX1 addition. Following induction of LTP, bath application of ZX1 did not affect fEPSP size or the PPF ratio (Figure S5C). Collectively, these results demonstrate that ZX1 does not block the expression of LTP of the mf-CA3 pyramid synapse (Figure S5C), implying that ZX1 inhibits induction of mf-CA3 LTP (Figures 3A and 3B).

Plasticity of mf-CA3 Pyramid Synapse in *ZnT3*$^{-/-}$ Mice

The availability of *ZnT3* null mutant mice (*ZnT3*$^{-/-}$) provides an additional approach to examine the role of vesicular zinc in plasticity of the mf-CA3 synapse (Cole et al., 1999). ZnT3 is a transporter required for packaging zinc into synaptic vesicles of the mossy fibers (Cole et al., 1999). In contrast to *mocha* mice in which vesicular zinc in the mf is reduced (Stoltenberg et al., 2004), vesicular zinc is eliminated altogether from the mf in *ZnT3*$^{-/-}$ mice (Cole et al., 1999). The findings with ZX1 led us to test two predictions: (1) that mf- LTP will be impaired in slices from *ZnT3*$^{-/-}$ compared to WT controls, and (2) that HFS of the mf will induce a reduction of PPF in slices from WT but not *ZnT3*$^{-/-}$ mice. We evaluated these predictions using whole cell recordings of CA3 pyramids. Whole-cell recordings of CA3 pyramids revealed no significant differences between WT and *ZnT3*$^{-/-}$ mice with respect to resting membrane potential, input resistance, capacitance, and time constant of decay (Table S3). HFS of the mf in slices from WT mice induced an increase of the EPSC of 167% ± 14% compared to baseline (n = 17, p = 0.0002; Figure 4, top left). A significant reduction of PPF was evident in CA3 pyramids following HFS (before HFS 3.1 ± 0.3; after HFS 2.1 ± 0.2, p = 0.002; Figure 4, bottom left). Contrary to our prediction, HFS of the mf in slices of *ZnT3*$^{-/-}$ mice induced an increase of the EPSC of 180% ± 15% compared to baseline (n = 14, p = 0.0001, Figure 4, top left), an effect similar to that observed in WT mice. Whereas the results with LTP were unexpected, the effects of HFS on PPF in *ZnT3*$^{-/-}$ mice conformed to our predictions. That is, HFS of the mf in slices from *ZnT3*$^{-/-}$ mice failed to induce a significant reduction of PPF (before HFS 2.7 ± 0.3; after HFS 2.6 ± 0.2, p = 0.49; Figure 4, bottom right). The HFS-mediated induction of mf-LTP in the absence of reductions of PPF in slices from *ZnT3*$^{-/-}$ mice was confirmed in additional experiments utilizing field potential recordings (Figure S6).

The association of mf-LTP with reduced ppf in WT but not *ZnT3*$^{-/-}$ mice supports a presynaptic locus of expression of

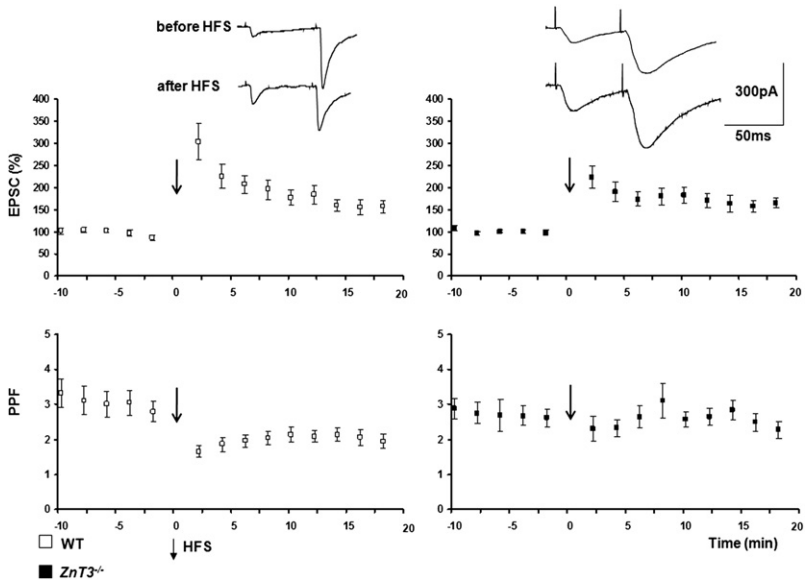

Figure 4. Divergent Effects of HFS on LTP and PPF of mf-CA3 Synapse in Slices of WT and *ZnT3*$^{-/-}$ Mice

Whole-cell recordings of CA3 pyramids were performed in hippocampal slices acutely isolated from WT or *ZnT3*$^{-/-}$ mice and the effects on LTP and PPF of mf-CA3 synapse were examined following HFS of the mossy fibers. Percent LTP induced by HFS: WT 167% ± 14% (n = 17, p = 0.0001; left top); *ZnT3*$^{-/-}$ 180% ± 15% (n = 14, p = 0.0001; right top). PPF before and 10–30 min after HFS: WT 3.1 ± 0.3 and 2.1 ± 0.2 (paired t test, p = 0.0002); *ZnT3*$^{-/-}$ 2.7 ± 0.3 and 2.6 ± 0.2 (paired t test, p = 0.5). Arrows denote the time of the application of HFS. The representative traces are averages of responses collected at intervals of 30 s for the 10 min preceding HFS (before) and the last 10 min of the recording following HFS (after); the interval between the pair of stimulations was 60 ms. Values represent mean ± standard error of the mean. See also Figure S6.

LTP in WT but not in *ZnT3*$^{-/-}$ mice. To obtain independent evidence in support of this interpretation, additional experiments examined spontaneous release of glutamate in the presence of tetrodotoxin (TTX), which eliminates action potentials; the action potential-independent release of glutamate detected as mEPSCs measures random monoquantal release of glutamate. The occurrence of increased frequency without change in amplitude of mEPSCs accompanying mf-LTP provides additional evidence of increased release of glutamate and a presynaptic locus of expression of mf-LTP (Kamiya et al., 2002). mEPSCs in CA3 pyramids (Jonas et al., 1993) were examined in whole-cell recordings in the presence of tetrodotoxin (1 μM). After recording synaptically evoked responses in the absence of TTX, TTX was added to the perfusion solution and control data were obtained after synaptically evoked responses were eliminated. Following collection of control data, TTX was removed from the perfusion solution; once synaptically evoked responses were restored, HFS was applied, and soon thereafter TTX was again added to the perfusion solution. HFS of the mf in slices from WT mice induced an increase of mEPSC frequency (before HFS 3.2 ± 0.5 Hz; after HFS 4.2 ± 0.6 Hz; n = 15; paired t test, p = 0.04) but no change in amplitude (amplitude before HFS, 35.4 ± 2.6 pA; after HFS 36 ± 2.4 pA; n = 15, paired t test, p = 0.44; Figure 5, left). By contrast, HFS of the mf in slices from *ZnT3*$^{-/-}$ mice induced a significant decrease of frequency (before HFS 5.3 ± 0.7 Hz; after HFS 3.0 ± 0.6 Hz; n = 6, paired t test, p = 0.05) and a significant increase of amplitude (before HFS 28 ± 4.3 pA; after HFS 34.7 ± 4.9 pA; n = 6, paired t test, p = 0.02; Figure 5, right). Notably, significant differences in frequency (WT 3.2 ± 0.5 Hz; *ZnT3*$^{-/-}$ 5.3 ± 0.7 Hz, t test, p = 0.02) but not amplitude (WT 35.4 ± 2.6 pA, n = 15; *ZnT3*$^{-/-}$ 28 ± 4.3 pA, n = 6, t test p = 0.08) of mEPSCs were evident between WT and *ZnT3*$^{-/-}$ mice prior to HFS. Importantly, differences of mEPSCs between WT and *ZnT3*$^{-/-}$ mice prior to HFS were not sufficient to account for the different effects of HFS because subsets of WT and *ZnT3*$^{-/-}$ mice with similar mEPSC amplitude and frequency at baseline exhibited divergent responses to HFS like that of the entire groups (not shown). Together with the HFS-induced reduction of PPF, the HFS-induced increased frequency of mEPSCs reinforces increased P_r as the mechanism underlying expression of mf-LTP in WT mice. By contrast, together with the failure of HFS to induce reductions of PPF, the HFS-induced decrease in frequency and increase in amplitude of mEPSCs implicates a postsynaptic locus underlying expression of mf-LTP in *ZnT3*$^{-/-}$ animals.

Locus of Induction of mf-LTP Is Postsynaptic in *ZnT3*$^{-/-}$ Mice

The evidence implicating presynaptic and postsynaptic loci underlying expression of mf-LTP in WT and *ZnT3*$^{-/-}$ animals, respectively, led us to ask whether the locus underlying induction of LTP also differed. In contrast to the unanimity that the locus of expression of LTP of this synapse is presynaptic in WT animals, controversy exists as to whether calcium-dependent events intrinsic to CA3 pyramids (postsynaptic) or mf terminals (presynaptic) mediate induction of mf-LTP (reviewed by Nicoll and Schmitz, 2005). To address this question, we examined the effects of dialyzing the postsynaptic cell with the calcium chelator BAPTA (50 mM) on induction of mf-LTP. In slices from WT animals, dialyzing a CA3 pyramid with BAPTA did not inhibit induction of LTP (Figure 6, top panel). In contrast, BAPTA inhibited induction of mf-LTP in slices from *ZnT3*$^{-/-}$ mice (Figure 6, middle panel). HFS of the mossy fibers in slices from *ZnT3*$^{-/-}$ mice induced an increase in the EPSC of 166 ± 16% (n = 12, paired t test, p = 0.001) in vehicle dialyzed CA3 pyramids, but only 123% ± 11% (n = 6, paired t test, p = 0.19 versus before HFS) in BAPTA dialyzed CA3 pyramids (Figure 6, middle). We conclude that chelation of intracellular calcium within postsynaptic CA3 pyramids inhibits induction of mf-LTP in slices from *ZnT3*$^{-/-}$ but not WT mice.

Zinc Inhibits Postsynaptic LTP at the mf-CA3 Synapse

One explanation for a postsynaptic locale underlying induction of mf-LTP in *ZnT3*$^{-/-}$ mice is that vesicular zinc inhibits

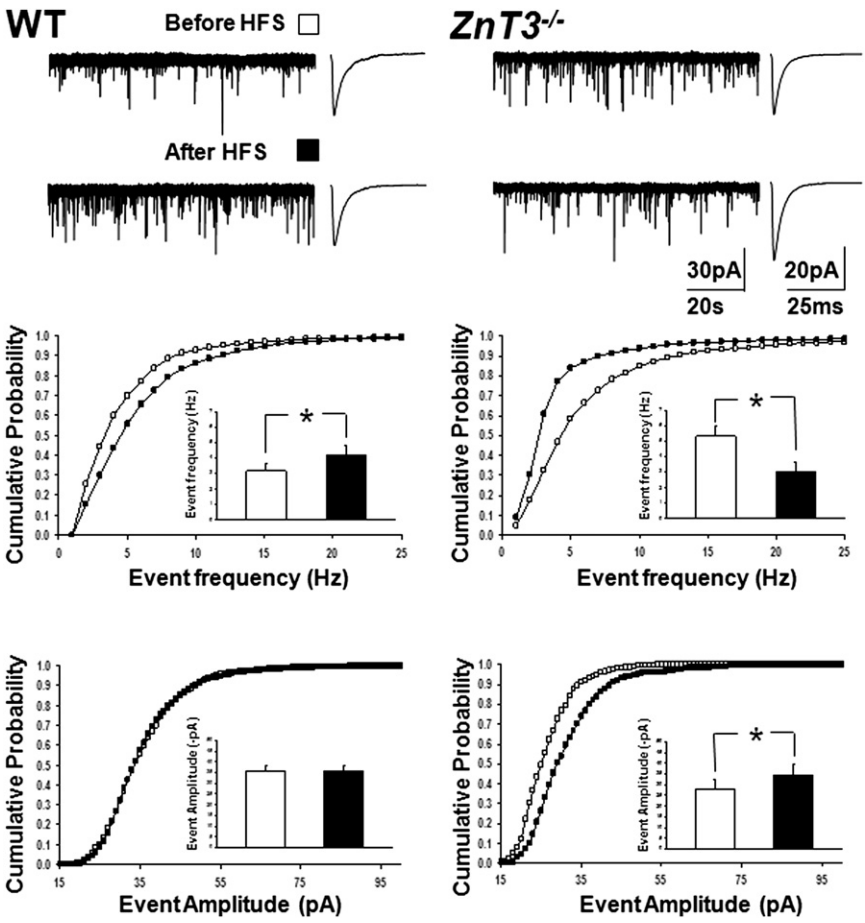

Figure 5. Analysis of mEPSCs Accompanying mf-CA3 LTP

mEPSCs accompanying mf-CA3 LTP were examined in slices of WT and *ZnT3*$^{-/-}$ mice. Top panels present results from representative slices before (basal) and approximately 15 min after HFS. Traces reflect recordings of epochs of at least 1 min as well as an average of the individual mEPSCs within the epoch. Middle and bottom panels present cumulative probability of event frequency and amplitude, respectively, with insets displaying mean ± SEM. In WT, HFS increased the frequency without change of amplitude of mEPSCs (left middle and bottom panels, respectively) as evident in significant increase of event frequency (mean ± SEM) from 3.2 ± 0.5 Hz recorded in 10 min epoch prior to HFS compared to 4.2 ± 0.6 Hz recorded 10–30 min after HFS (n = 15, paired t test, p = 0.04). In *ZnT3*$^{-/-}$, HFS decreased the event frequency and increased the event amplitude of mEPSCs (right middle and bottom panels, respectively) as evident in a decrease of frequency from 5.3 ± 0.7 Hz to 3.0 ± 0.6 Hz (mean ± SEM, n = 6, paired t test, p = 0.05); the amplitude increased from 28 ± 4.3 pA to 34.7 ± 4.9 pA after HFS (n = 6, paired t test, p = 0.02).

postsynaptic mf-LTP in WT mice. If so, chelation of zinc with ZX1 would be expected to reveal a postsynaptic mf-LTP in WT mice. To test this possibility, we examined the effects of dialyzing a CA3 pyramid with BAPTA on mf-LTP in the presence of ZX1 (100 μM) in the bath. In the presence of ZX1, dialyzing a CA3 pyramid with BAPTA abolished mf-LTP in slices from WT mice (Figure 6, bottom). With ZX1 (100 μM) in the bath, HFS of mf induced an increase in the EPSC of 134% ± 20% (n = 9) in vehicle dialyzed CA3 pyramids, but a small decrease in the EPSC of 82% ± 7% (n = 5) in BAPTA dialyzed CA3 pyramids (p = 0.04, t test, vehicle versus BAPTA) (Figure 6, bottom). Notably, dialyzing CA3 pyramids with BAPTA inhibits mf-LTP in the presence, but not the absence, of ZX1 in the bath (Figure 6, bottom). Thus inclusion of a chelator of extracellular zinc in the bath unmasked a postsynaptic locus for induction of mf-LTP in slices from WT mice.

To further test whether zinc inhibits postsynaptic LTP of the mf-CA3 synapse, we examined the effects of chelating extracellular zinc with ZX1 on the induction of mf-LTP in slices isolated from *rim1*α null mutant mice. The protein rim1α resides in the active zone of the presynaptic terminal and binds the synaptic vesicle protein, rab 3a; induction of mf-LTP is eliminated altogether in *rim1*α null mutant mice (Castillo et al., 2002). Confirming Castillo et al. (2002), with vehicle in the bath, we found that HFS of the mf did not induce LTP in slices from *rim1*α null mutant mice; a small nonsignificant decrease of fEPSP of 93% ± 11%, n = 4 when measured after 50–60 min compared to the 10 min immediately preceding HFS (Figure 7, top left). Remarkably, with ZX1 (100 μM) in the bath, HFS of the mf induced LTP in slices from *rim1*α null mutant mice. There was an increase of fEPSP of 151% ± 14%, n = 4, p = 0.016, vehicle versus ZX1 (Figure 7, top right). Notably, this mf-LTP was not accompanied by a reduction of paired pulse facilitation (Figure 7, bottom right). Thus, this extracellular zinc chelator partially inhibits induction of mf-LTP in WT mice (Figure 3, top left and right), yet promotes induction of mf-LTP in *rim1*α mutant mice (Figure 7, top left and right). That ZX1 promotes induction of mf-LTP in *rim1*α null mutant mice reinforces the conclusion that synaptically released zinc inhibits induction of postsynaptic mf-LTP.

DISCUSSION

We tested the hypothesis that vesicular zinc is required for mf-LTP. To evaluate this hypothesis, we synthesized an extracellular zinc chelator with selectivity and kinetic properties suitable for study of the large and rapid transient of zinc in the synaptic cleft induced by HFS of the mossy fibers. The results reveal that zinc is required for induction of presynaptic mf-LTP. Unexpectedly, vesicular zinc also inhibits induction of a novel form of postsynaptic mf-LTP. Because the mf-CA3 synapse conveys a powerful excitatory input to hippocampus, the unique dual control of its efficacy by zinc is critical to function of hippocampal circuitry in health and disease.

The discovery of a novel zinc chelator, ZX1, provided a valuable tool with which to examine the contribution of zinc to

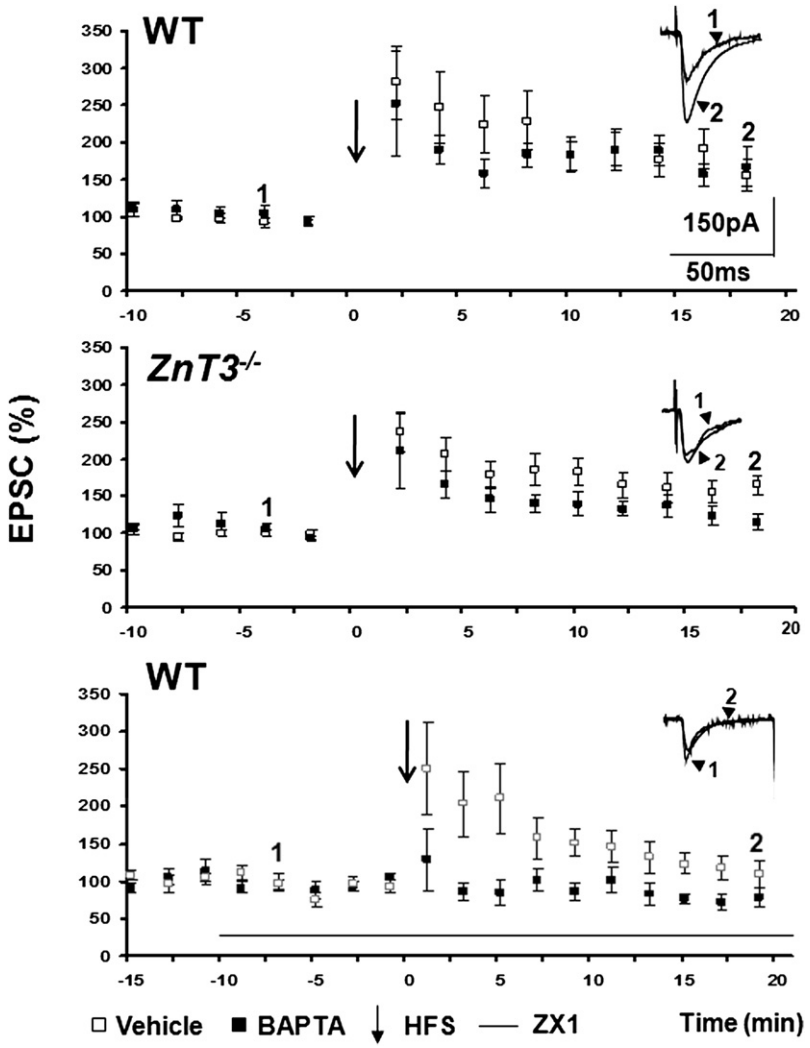

Figure 6. Effects of Dialyzing CA3 Pyramids with BAPTA on mf-CA3 LTP in *ZnT3*$^{-/-}$ and WT Mice

In WT in ACSF (top), the percent potentiation was similar when CA3 pyramids were dialyzed with BAPTA 171% ± 17% (n = 7) compared to vehicle 180% ± 22% (n = 8) (Student's t test, p = 0.8). In *ZnT3*$^{-/-}$ in ACSF (middle), the percent potentiation was reduced when CA3 pyramids were dialyzed with BAPTA 123% ± 11% (n = 6) compared to vehicle 166% ± 16% (n = 12; Student's t test, p = 0.009). The amount of potentiation in BAPTA dialyzed cells was significantly greater in WT compared to *ZnT3*$^{-/-}$ animals (t test, p = 0.04). In WT with ZX1 (100 μM) in the bath (bottom), the percent potentiation was eliminated when CA3 pyramids were dialyzed with BAPTA 82% ± 7% (n = 5) compared to vehicle 134% ± 20% (n = 9) (t test, p = 0.04); note that data of vehicle dialyzed CA3 pyramids with ZX1 in bath are reprinted from experiment presented in Figure 3 (right middle). Arrows denote the time of application of HFS and arrowheads denote the baseline EPSC (1) and the EPSC after HFS (2) for BAPTA experiments. Values represent mean ± standard error of the mean.

mf-LTP. Dipicolylamine (DPA) was selected as the primary zinc-binding unit, because it selectively coordinates zinc, as demonstrated by a number of zinc fluorescence or MRI sensors (Chang and Lippard, 2006; Burdette et al., 2001; Zhang et al., 2007). As revealed by potentiometric titrations, the nitrogen-rich ligand environment renders ZX1 selective for zinc over potassium, calcium, and magnesium, major intra- and extracellular free cations. Although ZX1 binds other endogenous transition metal ions, such as copper, iron, and manganese, the levels of these redox-active species as free ions in the cell are strictly regulated to be quite low. Consistent with this idea, Timm's stain for transition metal ions is eliminated in the hippocampus of *ZnT3*$^{-/-}$ mice (Cole et al., 1999), implying that zinc is the only transitional metal ion present in sufficiently high concentrations to be detected. The rapidity of binding zinc together with its high affinity for zinc ($K_d \approx 10^{-9}$ M) allowed us to estimate that ZX1 successfully chelated the majority of the bolus of free zinc that is present in the synaptic cleft following its HFS-induced release from mf terminals. Although technical limitations preclude direct measures of zinc within the synaptic cleft itself, the peak zinc concentration is thought to approximate 100 μM, an estimate based upon zinc-mediated inhibition of a synaptic I_{NMDA} in a CA3 pyramid evoked by mf stimulation (Vogt et al., 2000). Using kinetic and binding affinity data determined experimentally in the present work (Figures 2 and S4), we compute that virtually all of the 100 μM maximum concentration levels present transiently within the synaptic cleft would be chelated by 100 μM ZX1 under the experimental conditions employed in this study. The fact that inhibition of mf-LTP by 100 μM and 200 μM ZX1 is nearly identical (Figure 3, top right) is consistent with this prediction. ZX1 provides two major advantages over CaEDTA, the most commonly used reagent to chelate extracellular zinc, namely, selectivity and rate of zinc binding. Although EDTA binds zinc with high affinity ($K_d \approx 10^{-15}$ M), EDTA also tightly binds calcium and magnesium. The use of the monocalcium complex (CaEDTA), rather than EDTA alone, is aimed at avoiding perturbation of extracellular calcium homeostasis. Nevertheless, because the extracellular concentrations of calcium and magnesium are approximately 2 mM, concentrations of CaEDTA used to study mf-LTP (2.5–10 mM) jeopardize the homeostasis of both extracellular calcium and magnesium. The excessive buffering of divalent cations may contribute to unstable whole-cell recordings observed with CaEDTA (Li et al., 2010). With respect to zinc itself, the affinities of CaEDTA and ZX1 are similar (1.6 and 1 nM, respectively) yet the *rate* of zinc chelation by ZX1 is about an order of magnitude faster than that for CaEDTA (Table S2). The greater rapidity of zinc chelation by ZX1 presumably underlies the successful disinhibition of the synaptically evoked high affinity I_{NMDA} of CA3 pyramid by ZX1 but not CaEDTA (Figure 2C). Collectively, the slow kinetics of zinc chelation together with lack of ion selectivity may explain the conflicting results reported with respect to the use of CaEDTA to modulate mf-LTP (Vogt et al., 2000; Li et al.,

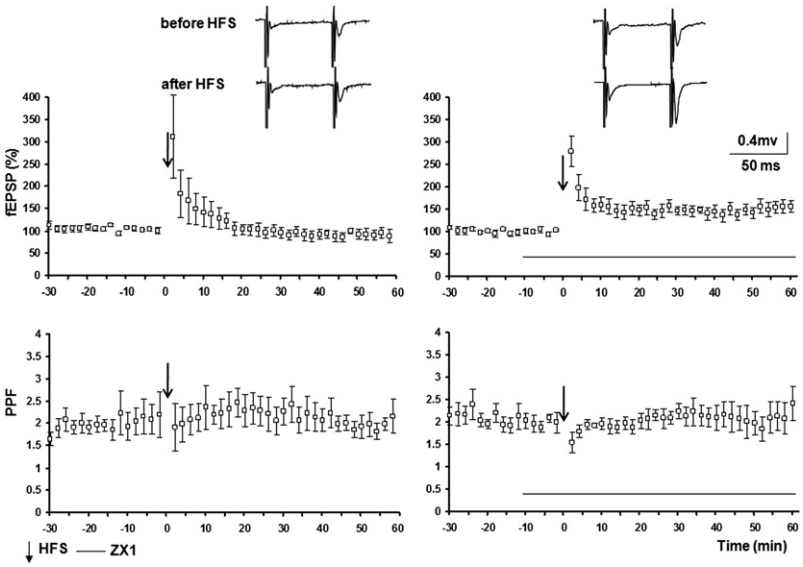

Figure 7. ZX1 Disinhibits mf-LTP in rim1α Null Mutant Mice

In rim1α null mutant mice, HFS of the mf did not induce LTP as detected in field potential recordings in presence of ACSF (a small nonsignificant decrease of fEPSP of 93% ± 11%, n = 4 when measured 50–60 min after compared to the 10 min immediately preceding HFS; left panel). By contrast, with ZX1 (100 μM) in the bath, HFS of the mf induced LTP in slices from rim1α null mutant mice (an increase of fEPSP of 151% ± 14%, n = 4, p = 0.016, vehicle versus ZX1; right panel); this mf-LTP was not accompanied by a reduction of paired pulse facilitation (bottom right). The representative traces are averages of responses collected at intervals of 30 s for the 10 min preceding HFS (before) and the last 10 min of the recording following HFS (after); the interval between the pair of stimulations was 60 ms. Values represent mean ± standard error of the mean.

2001; Huang et al., 2008). By contrast, the rapid kinetics of zinc chelation together with its ion selectivity render ZX1 a valuable tool for study of the large and rapid transient of zinc within the synaptic cleft induced by mf stimulation.

The application of ZX1 has revealed a critical role for zinc induction of this classic form of presynaptic LTP in WT animals. There is universal agreement that the expression of mf-LTP is caused by an increase of glutamate release (reviewed by Henze et al., 2000 and Nicoll and Schmitz, 2005). This assertion is based upon findings that mf-LTP is accompanied by reductions of PPF, increased frequency but not amplitude of mEPSCs, and increased rate of use dependent block by MK-801 (Zalutsky and Nicoll, 1990; Tong et al., 1996; Weisskopf and Nicoll, 1995). That genetic deletion of each of two presynaptic proteins, rab3a and rim1α, eliminates mf-LTP provides additional support for a presynaptic locus (Castillo et al., 1997; Castillo et al., 2002). Our findings that mf-LTP in vehicle-treated WT slices is associated with reduced PPF and an increased mEPSC frequency without a change in amplitude is consistent with these previous findings. The discovery that ZX1 not only inhibits mf-LTP but also prevents the reduction of PPF in WT animals implicates zinc as a critical factor responsible for induction of this presynaptic plasticity. This conclusion was reinforced by studies of *ZnT3*$^{-/-}$ mice lacking vesicular zinc in which mf-LTP was induced without an accompanying reduction of PPF. Further evidence of a requirement for vesicular zinc for this presynaptic plasticity is that mf-LTP in WT mice is associated with an increased frequency of mEPSCs, but in *ZnT3*$^{-/-}$ mice with a reduced frequency and increased amplitude of mEPSCs.

One unexpected and important outcome is that vesicular zinc also inhibits induction of postsynaptic mf-LTP. The assertion that vesicular zinc masks postsynaptic mf-LTP is based on two findings. One is that mf-LTP can be induced in *ZnT3*$^{-/-}$ mice without reduction of PPF and with increased amplitude and decreased frequency of mEPSCs; these results diverge sharply from mf-LTP in WT animals. The second is that ZX1, a chelator of extracellular zinc, unmasks mf-LTP in *rim1α* null mutant mice which lack presynaptic mf-LTP (Castillo et al., 2002); that mf-LTP in ZX1 treated slices of *rim1α* null mutant mice is not accompanied by a reduction of PPF is consistent with a postsynaptic locus of expression of mf-LTP in this condition. The locus of induction of mf-LTP in the absence of vesicular zinc also resides postsynaptically, because the mf-LTP evident in *ZnT3*$^{-/-}$ mice was inhibited by dialyzing CA3 pyramids with BAPTA. Similarly, the residual mf-LTP detected in WT mice in the presence of ZX1 was inhibited by dialyzing CA3 pyramids with BAPTA. These findings differ from mf-LTP in WT animals induced in the presence of ACSF, which was not inhibited by dialyzing CA3 pyramids with BAPTA. Notably, the magnitude of the mf-LTP observed in the *ZnT3*$^{-/-}$ and ZX1-treated *rim1α*$^{-/-}$ slices exceeded that evident in the ZX1-treated slices from WT animals; the lifelong presence of the mutations in the *ZnT3*$^{-/-}$ and the *rim1α*$^{-/-}$ may have permitted emergence of homeostatic mechanisms not present when ZX1 is acutely applied to a slice from a WT mouse. Finally, inclusion of APV throughout these experiments implies that induction and expression of this postsynaptic mf-LTP occurs independently of NMDA receptors and thus differs from a postsynaptic mf-LTP described by Kwon and Castillo (2008) and Rebola et al. (2008). The mechanisms underlying induction and expression of this novel form of postsynaptic mf-LTP remain to be determined.

What is the locale at which vesicular zinc promotes the increased glutamate P_r underlying mf-LTP in WT animals? The finding that dialyzing CA3 pyramids with BAPTA inhibits induction of mf-LTP in slices from WT mice in the presence of ZX1 or in slices from *ZnT3*$^{-/-}$ mice points to a presynaptic locus underlying induction of mf-LTP in WT animals in the presence of ACSF. That is, the inhibition of mf-LTP by BAPTA implies that sufficient concentrations of BAPTA are diffusing through the dendritic tree of CA3 pyramids to chelate calcium required for induction of mf-LTP under the conditions of these experiments. The ineffectiveness of BAPTA in inhibiting mf-LTP in WT slices in ACSF supports the conclusion that events underlying induction reside presynaptically within mf terminals.

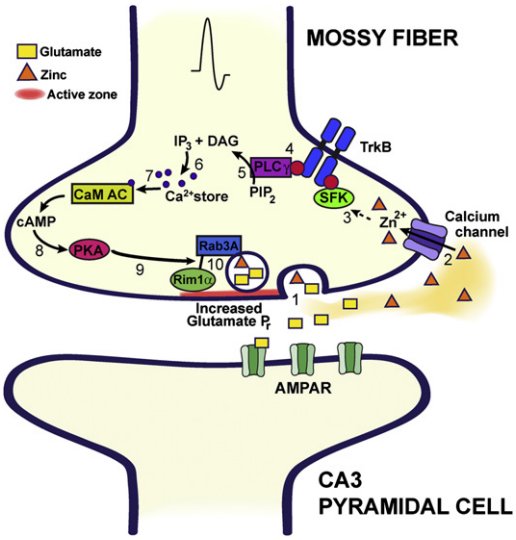

Figure 8. Model Proposing How Vesicular Zinc Promotes Increased Glutamate P_r Underlying Presynaptic mf-CA3 LTP

Invasion of mossy terminal by a high frequency train of action potentials results in calcium influx and fusion of synaptic vesicles with the terminal plasma membrane (1), resulting in release of zinc into synaptic cleft. The synaptically released zinc reenters the same or nearby presynaptic terminal through a voltage-gated calcium channel (2). The local elevation of zinc concentration within the terminal activates a src family kinase (3) which phosphorylates and promotes activation of TrkB, one consequence of which is the phosphorylation and activation of PLCγ1 (4). PLCγ1 in turn catalyzes cleavage of phosphatidyl inositol bisphosphate (PIP_2, leading to formation of diacyl glycerol (DAG) and inositol 3,4,5 phosphate (IP_3) (5). IP_3 binds to and triggers release of calcium from endoplasmic reticulum (6), resulting in activation of calcium-calmodulin adenylate cyclase (Ca-CaM AC) (7), formation of cAMP, and activation of protein kinase A (8). Subsequent steps include interaction of the synaptic vesicle associated protein, rab3A, and its partner in the active zone, rim1α (9), the net result being an increased glutamate P_r (10). This proposal is based in part upon the finding that zinc is capable of activating TrkB and its downstream signaling independently of brain-derived neurotrophic factor (BDNF) (Huang et al., 2008; Huang and McNamara, 2010). Inhibition of TrkB kinase prevents induction of mf-LTP (Huang et al., 2008) as well as the accompanying reduction of PPF (unpublished data). Preventing TrkB activation of PLCγ1 signaling inhibits induction of mf-CA3 LTP (He et al., 2010) and the accompanying reduction of PPF (unpublished data). Because activation of $PLC_{\gamma 1}$ results in formation of IP3 and release of calcium from the endoplasmic reticulum, this model is consistent with the inhibition of mf-CA3 LTP by presynaptic calcium chelation with EGTA (Tong et al., 1996) and by genetic or pharmacological inhibition of α1E-containing calcium channels (Breustedt et al., 2003; Dietrich et al., 2003). This model is also consistent with evidence that TrkB activation promotes transmitter release from presynaptic terminals (Jovanovic et al., 2000; Tyler et al., 2002; Lohof et al., 1993). The requirements of the synaptic vesicle protein, rab3a, and its interacting partner, rim1α, for induction of mf-CA3 LTP (Castillo et al., 1997; Castillo et al., 2002) suggest that TrkB-activated $PLC_{\gamma 1}$ signaling somehow interacts with these molecular components of the release apparatus to promote increased P_r and LTP. A requirement for rab3a in the BDNF-mediated increase of mEPSC frequency in hippocampal neurons supports this suggestion (Alder et al., 2005).

Whether the locus of induction of mf-LTP is pre- or postsynaptic has been controversial (reviewed by Henze et al., 2000 and Nicoll and Schmitz, 2005), but our conclusion is consistent with evidence implicating a presynaptic locus (Tong et al., 1996).

Our interpretation that vesicular zinc acts presynaptically raises the question as to what molecular consequences are triggered by the ion that culminate in the increased glutamate P_r that underlies mf-LTP in WT animals. We propose that vesicular zinc, released by HFS of the mf, reenters the mf terminals where it triggers a chain of molecular events. One possibility is that increased concentrations of zinc in the cytosol of the presynaptic terminal transactivate the receptor tyrosine kinase, TrkB (Huang et al., 2008; Figure 8). This model is consistent with evidence that TrkB activation can promote transmitter release from presynaptic terminals (Jovanovic et al., 2000; Tyler et al., 2002; Lohof et al., 1993), that TrkB kinase activity is required for mf-LTP (Huang et al., 2008), and that zinc can transactivate TrkB (Huang et al., 2008). Rapid chelation of synaptically released zinc by ZX1 would inhibit such a process.

Our findings establish two important functions for zinc that is localized to synaptic vesicles of the hippocampal mfs: zinc promotes the increased P_r that underlies presynaptic mf-LTP and it also masks induction of postsynaptic mf-LTP. Context-dependent fear conditioning is one behavior potentially related to presynaptic mf-LTP in particular because defects in this behavior have been identified in young adult *ZnT3* null mutant mice and following injection of a zinc chelator locally in CA3 of WT mice (Sindreu et al., 2011). Emergence of a postsynaptic mf-LTP may help explain the absence of detectable deficits in multiple behaviors examined in young adult *ZnT3* null mutant mice (Cole et al., 2001; Adlard et al., 2010). It seems plausible that dual control of the mf-CA3 synapse by vesicular zinc supports the physiological functions subserved by this synapse while limiting pathologic hyperexcitability mediated by excessive activation of CA3 pyramids. Future investigations will seek to determine the molecular mechanisms underlying these dual functions and whether vesicular zinc exerts similar actions in diverse association cortical circuits in addition to the mf-CA3 synapse.

EXPERIMENTAL PROCEDURES

Preparation and Characterization of ZX1

Full details of the preparation, characterization, and physical properties of the new chelator are provided in Supplemental Information. The compound can be obtained from Strem Chemical Co.

Potentiometric Titrations

Potentiometric titrations were performed on a Mettler-Toledo T70 autotitrator, operated by the LabX-light software. A pH glass electrode (DG111-SC), applied for pH measurements was calibrated with standard buffers (pH 4, 7, 10) prior to use. All solutions were degassed to avoid CO_2 contamination. The titrant (0.1 M NaOH,) was calibrated with analytically pure, crystalline potassium hydrogen phthalate (KHP). The titration experiments were run at 25°C controlled by a circulating thermostatted bath. The ionic strength was fixed with 100 mM KCl. Data analysis and calculation of association constants were performed with HYPERQUAD software.

Kinetic Studies

All kinetic measurements were performed in pH 7 buffered solutions containing 50 mM of PIPES and 100 mM KCl. Millipore purified water was used to prepare all aqueous solutions. A glass electrode (Orion, Boston), calibrated before each use, was employed to determine solution pH. The kinetics of fluorescence quenching experiment was performed on a Photon Technology International (Lawrenceville, NJ) Quanta Master 4 L-format scanning spectrofluorimeter equipped with an LPS-220B 75-W xenon lamp and power supply,

an A-1010B lamp housing with integrated igniter, a switchable 814 photon-counting/analog photomultiplier detection unit, and a MD-5020 motor driver. Samples were held in 1 × 1 cm quartz cuvettes (3.5 ml volume, Starna, Atascadero, CA). The kinetic traces were obtained by following fluorescence emission at 515 nm (λ_{ex} = 494 nm); the fluorescence was recorded every one second for a total of 600 s. Double-mixing stopped-flow kinetics studies were performed with a Hi-Tech SF-61 DX2 apparatus equipped with fluorescence detection. Excitation was provided at 494 nm. A GG455 glass cutoff filter (<455 nm) was placed over the exit to the photomultiplier tube, and emission was monitored from 455 to 700 nm. The observed rate constants obtained from all sets of experiments were calculated by employing the Kinet-Assyst software package (HiTech) to fit individual traces to single exponentials.

Mice

ZnT3 null mutant mice, obtained from Dr. Richard Palmiter, University of Washington, were generated by crossing male and female heterozygotes maintained on a C57BL/6 background (Cole et al., 1999). The genotype of each animal was verified twice using PCR of genomic DNA isolated from tail before and after experiments.

Hippocampal Slice Preparation and Electrophysiological Recording

Mice were anaesthetized with pentobarbital and decapitated, and hippocampal slices prepared for electrophysiological study. A bipolar tungsten-stimulating electrode was placed near the junction of the granule cell layer and hilus near the midpoint of the suprapyramidal blade of the dentate. Synaptic events were evoked by a stimulus pulse; 0.2 ms monopolar square pulses were delivered at 0.033 Hz with a Digitmer constant current stimulator (DS3, Digitimer Ltd. UK). Data were collected from slices at room temperature using a Multi 700A amplifier and pClamp 9.2 software (Molecular Devices, Sunnyvale, CA). Details of field potential and whole-cell recordings for assessment of mf-LTP are provided in Supplemental Experimental Procedures.

To be considered a mossy fiber excitatory postsynaptic event (fEPSP or EPSC), the following criteria were applied: (1) the ratio for paired pulse facilitation (PPF) at 60 ms interval was $\geq$ 1.75; (2) frequency facilitation at 20 Hz was $\geq$2.0 as determined by the ratio of the amplitude of the response to the third pulse compared to the first pulse (Toth et al., 2000); and (3) application of the Group II metabotropic glutamate receptor (mGluR) II agonist 2-(2,3-dicarboxycyclopropy) glycine (DCG-IV; 1 μM) at the end of the experiment reduced the amplitude of the evoked fEPSP or EPSC by $\geq$70%.

SUPPLEMENTAL INFORMATION

Supplemental Information includes Supplemental Experimental Procedures, six figures, and three tables and can be found with this article online at doi:10.1016/j.neuron.2011.07.019.

ACKNOWLEDGMENTS

This work was supported by a grant from the National Institute of General Medical Sciences (GM065519 to S.J.L.) and from the National Institute of Neurological Disease and Stroke (NS56217 to J.O.M.). The authors thank Drs. Daniela Buccella, Nicole Calakos, Danny Jones, and Richard Mooney for valuable discussions and Wei-Hua Qian for support of mouse husbandry and genotyping.

Accepted: July 15, 2011
Published: September 21, 2011

REFERENCES

Adlard, P.A., Parncutt, J.M., Finkelstein, D.I., and Bush, A.I. (2010). Cognitive loss in zinc transporter-3 knock-out mice: a phenocopy for the synaptic and memory deficits of Alzheimer's disease? J. Neurosci. *30*, 1631–1636.

Alder, J., Thakker-Varia, S., Crozier, R.A., Shaheen, A., Plummer, M.R., and Black, I.B. (2005). Early presynaptic and late postsynaptic components contribute independently to brain-derived neurotrophic factor-induced synaptic plasticity. J. Neurosci. *25*, 3080–3085.

Bliss, T.V.P., and Collingridge, G.L. (1993). A synaptic model of memory: long-term potentiation in the hippocampus. Nature *361*, 31–39.

Breustedt, J., Vogt, K.E., Miller, R.J., Nicoll, R.A., and Schmitz, D. (2003). α1E-containing Ca^{2+} channels are involved in synaptic plasticity. Proc. Natl. Acad. Sci. USA *100*, 12450–12455.

Budde, T., Minta, A., White, J.A., and Kay, A.R. (1997). Imaging free zinc in synaptic terminals in live hippocampal slices. Neuroscience *79(2)*, 347–358.

Burdette, S.C., Walkup, G.K., Spingler, B., Tsien, R.Y., and Lippard, S.J. (2001). Fluorescent sensors for Zn^{2+} based on a fluorescein platform: synthesis, properties and intracellular distribution. J. Am. Chem. Soc. *123*, 7831–7841.

Castillo, P.E., Janz, R., Südhof, T.C., Tzounopoulos, T., Malenka, R.C., and Nicoll, R.A. (1997). Rab3A is essential for mossy fibre long-term potentiation in the hippocampus. Nature *388*, 590–593.

Castillo, P.E., Schoch, S., Schmitz, F., Südhof, T.C., and Malenka, R.C. (2002). RIM1α is required for presynaptic long-term potentiation. Nature *415*, 327–330.

Chang, C.J., and Lippard, S.J. (2006). Zinc metalloneurochemistry: physiology, pathology, and probes. In Metal Ions in Life Sci., *Volume 1*, A. Sigel, H. Sigel, and R.K.O. Sigel, eds. (Chichester, UK: John Wiley & Son, Ltd), pp. 321–370.

Chang, C.J., Nolan, E.M., Jaworski, J., Burdette, S.C., Sheng, M., and Lippard, S.J. (2004). Bright fluorescent chemosensor platforms for imaging endogenous pools of neuronal zinc. Chem. Biol. *11*, 203–210.

Choi, Y.B., and Lipton, S.A. (1999). Identification and mechanism of action of two histidine residues underlying high-affinity Zn^{2+} inhibition of the NMDA receptor. Neuron *23*, 171–180.

Cole, T.B., Wenzel, H.J., Kafer, K.E., Schwartzkroin, P.A., and Palmiter, R.D. (1999). Elimination of zinc from synaptic vesicles in the intact mouse brain by disruption of the *ZnT3* gene. Proc. Natl. Acad. Sci. USA *96*, 1716–1721.

Cole, T.B., Martyanova, A., and Palmiter, R.D. (2001). Removing zinc from synaptic vesicles does not impair spatial learning, memory, or sensorimotor functions in the mouse. Brain Res. *891*, 253–265.

Dietrich, D., Kirschstein, T., Kukley, M., Pereverzev, A., von der Brelie, C., Schneider, T., and Beck, H. (2003). Functional specialization of presynaptic Cav2.3 Ca^{2+} channels. Neuron *39*, 483–496.

Frederickson, C.J., Koh, J.Y., and Bush, A.I. (2005). The neurobiology of zinc in health and disease. Nat. Rev. Neurosci. *6*, 449–462.

Haug, F.M.S. (1967). Electron microscopical localization of the zinc in hippocampal mossy fibre synapses by a modified sulfide silver procedure. Histochemie *8*, 355–368.

He, X.P., Pan, E., Sciarretta, C., Minichiello, L., and McNamara, J.O. (2010). Disruption of TrkB-mediated phospholipase Cγ signaling inhibits limbic epileptogenesis. J. Neurosci. *30*, 6188–6196.

Henze, D.A., Urban, N.N., and Barrionuevo, G. (2000). The multifarious hippocampal mossy fiber pathway: a review. Neuroscience *98*, 407–427.

Huang, Y.Z., and McNamara, J.O. (2010). Mutual regulation of Src family kinases and the neurotrophin receptor TrkB. J. Biol. Chem. *285*, 8207–8217.

Huang, Y.Z., Pan, E., Xiong, Z.-Q., and McNamara, J.O. (2008). Zinc-mediated transactivation of TrkB potentiates the hippocampal mossy fiber-CA3 pyramid synapse. Neuron *57*, 546–558.

Jonas, P., Major, D., and Sakmann, B. (1993). Quantal components of unitary EPSCs at the mossy fibre synapse on CA3 pyramidal cells of rat hippocampus. J. Physiol. *472*, 615–663.

Jovanovic, J.N., Czernik, A.J., Fienberg, A.A., Greengard, P., and Sihra, T.S. (2000). Synapsins as mediators of BDNF-enhanced neurotransmitter release. Nat. Neurosci. *3*, 323–329.

Kamiya, H., Umeda, K., Ozawa, S., and Manabe, T. (2002). Presynaptic Ca^{2+} entry is unchanged during hippocampal mossy fiber long-term potentiation. J. Neurosci. *22*, 10524–10528.

Kwon, H.B., and Castillo, P.E. (2008). Long-term potentiation selectively expressed by NMDA receptors at hippocampal mossy fiber synapses. Neuron *57*, 108–120.

Li, Y., Hough, C.J., Frederickson, C.J., and Sarvey, J.M. (2001). Induction of mossy fiber —> CA3 long-term potentiation requires translocation of synaptically released Zn^{2+}. J. Neurosci. *21*, 8015–8025.

Li, Y., Calfa, G., Inoue, T., Amaral, M.D., and Pozzo-Miller, L. (2010). Activity-dependent release of endogenous BDNF from mossy fibers evokes a TRPC3 current and Ca^{2+} elevations in CA3 pyramidal neurons. J. Neurophysiol. *103*, 2846–2856.

Lohof, A.M., Ip, N.Y., and Poo, M.M. (1993). Potentiation of developing neuromuscular synapses by the neurotrophins NT-3 and BDNF. Nature *363*, 350–353.

Malinow, R., and Malenka, R.C. (2002). AMPA receptor trafficking and synaptic plasticity. Annu. Rev. Neurosci. *25*, 103–126.

Maske, H. (1955). Topochemical detection of zinc in the Ammon's horn of different mammals. Naturwissenschaften *42*, 424.

Nicoll, R.A., and Schmitz, D. (2005). Synaptic plasticity at hippocampal mossy fibre synapses. Nat. Rev. Neurosci. *6*, 863–876.

Nolan, E.M., Jaworski, J., Okamoto, K.I., Hayashi, Y., Sheng, M., and Lippard, S.J. (2005). QZ1 and QZ2: rapid, reversible quinoline-derivatized fluoresceins for sensing biological Zn(II). J. Am. Chem. Soc. *127*, 16812–16823.

Paoletti, P., Ascher, P., and Neyton, J. (1997). High-affinity zinc inhibition of NMDA NR1–NR2A receptors. J. Neurosci. *17*, 5711–5725.

Qian, J., and Noebels, J.L. (2005). Visualization of transmitter release with zinc fluorescence detection at the mouse hippocampal mossy fibre synapse. J. Physiol. *566*, 747–758.

Quinta-Ferreira, M.E., and Matias, C.M. (2004). Hippocampal mossy fiber calcium transients are maintained during long-term potentiation and are inhibited by endogenous zinc. Brain Res. *1004*, 52–60.

Rebola, N., Lujan, R., Cunha, R.A., and Mulle, C. (2008). Adenosine A_{2A} receptors are essential for long-term potentiation of NMDA-EPSCs at hippocampal mossy fiber synapses. Neuron *57*, 121–134.

Regehr, W.A., and Stevens, C.F. (2001). Physiology of synaptic transmission and short-term plasticity. In Synapses, W.M. Cowan, T.C. Südhof, and C.F. Stevens, eds. (Baltimore, MD: The Johns Hopkins University Press).

Reid, C.A., Dixon, D.B., Takahashi, M., Bliss, T.V.P., and Fine, A. (2004). Optical quantal analysis indicates that long-term potentiation at single hippocampal mossy fiber synapses is expressed through increased release probability, recruitment of new release sites, and activation of silent synapses. J. Neurosci. *24*, 3618–3626.

Sindreu, C., Palmiter, R.D., and Storm, D.R. (2011). Zinc transporter ZnT-3 regulates presynaptic Erk1/2 signaling and hippocampus-dependent memory. Proc. Natl. Acad. Sci. USA *108*, 3366–3370.

Stoltenberg, M., Nejsum, L.N., Larsen, A., and Danscher, G. (2004). Abundance of zinc ions in synaptic terminals of *mocha* mutant mice: zinc transporter 3 immunohistochemistry and zinc sulphide autometallography. J. Mol. Histol. *35*, 141–145.

Tong, G., Malenka, R.C., and Nicoll, R.A. (1996). Long-term potentiation in cultures of single hippocampal granule cells: a presynaptic form of plasticity. Neuron *16*, 1147–1157.

Toth, K., Suares, G., Lawrence, J.J., Philips-Tansey, E., and McBain, C.J. (2000). Differential mechanisms of transmission at three types of mossy fiber synapse. J. Neurosci. *20*, 8279–8289.

Traynelis, S.F., Burgess, M.F., Zheng, F., Lyuboslavsky, P., and Powers, J.L. (1998). Control of voltage-independent zinc inhibition of NMDA receptors by the NR1 subunit. J. Neurosci. *18*, 6163–6175.

Tyler, W.J., Perrett, S.P., and Pozzo-Miller, L.D. (2002). The role of neurotrophins in neurotransmitter release. Neuroscientist *8*, 524–531.

Vogt, K., Mellor, J., Tong, G., and Nicoll, R. (2000). The actions of synaptically released zinc at hippocampal mossy fiber synapses. Neuron *26*, 187–196.

Weisskopf, M.G., and Nicoll, R.A. (1995). Presynaptic changes during mossy fibre LTP revealed by NMDA receptor-mediated synaptic responses. Nature *376*, 256–259.

Zalutsky, R.A., and Nicoll, R.A. (1990). Comparison of two forms of long-term potentiation in single hippocampal neurons. Science *248*, 1619–1624.

Zhang, X.A., Lovejoy, K.S., Jasanoff, A., and Lippard, S.J. (2007). Water-soluble porphyrins as a dual-function molecular imaging platform for MRI and fluorescence zinc sensing. Proc. Natl. Acad. Sci. USA *104*, 10780–10785.